

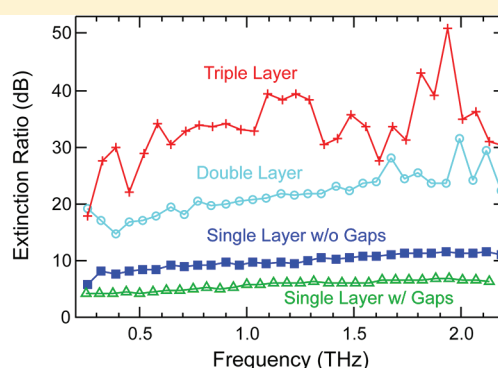
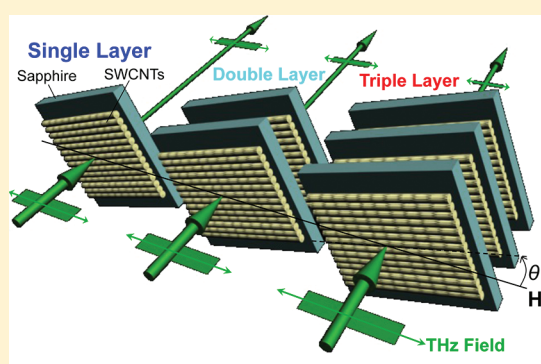
Broadband Terahertz Polarizers with Ideal Performance Based on Aligned Carbon Nanotube Stacks

Lei Ren,^{†,‡,#} Cary L. Pint,^{‡,§,#} Takashi Arikawa,^{†,‡} Kei Takeya,^{||} Iwao Kawayama,^{||} Masayoshi Tonouchi,^{||} Robert H. Hauge,[§] and Junichiro Kono^{*,†,‡}

[†]Department of Electrical and Computer Engineering, [‡]Department of Physics and Astronomy, and [§]Department of Chemistry, Rice University, Houston, Texas 77005, United States

^{||}Institute of Laser Engineering, Osaka University, Yamadaoka 2-6, Suita, Osaka 565-0871, Japan

S Supporting Information



ABSTRACT: We demonstrate a terahertz polarizer built with stacks of aligned single-walled carbon nanotubes (SWCNTs) exhibiting ideal broadband terahertz properties: 99.9% degree of polarization and extinction ratios of 10^{-3} (or 30 dB) from ~ 0.4 to 2.2 THz. Compared to structurally tuned and fragile wire-grid systems, the performance in these polarizers is driven by the inherent anisotropic absorption of SWCNTs that enables a physically robust structure. Supported by a scalable dry contact-transfer approach, these SWCNT-based polarizers are ideal for emerging terahertz applications.

KEYWORDS: Terahertz polarizer, aligned carbon nanotubes, chemical vapor deposition, contact transfer

Applications in terahertz (THz) technology are progressing at a rapid rate in concert with new compact techniques to produce THz radiation.^{1–5} The potential applications of THz technology are diverse, as THz radiation provides a unique medium for noninvasive imaging, communications, and sensing devices that are currently being developed on both a research and industrial scale.^{1,2} Complementary to the development of this technology, it is not only important to devise ways to produce THz radiation but also to have robust approaches to manipulate it and extract the detailed information contained within a coherent THz pulse. Currently, a host of wire-grid structures composed of uniformly spaced metal wires are employed as polarizers and filters for THz applications. Although these exhibit high extinction coefficients at THz wavelengths (>25 dB), they have drawbacks of fragility and a structurally tuned architecture that is not extendable to broadband THz operation. Conventional THz polarizers are made by mechanically winding thin metallic strings, such as tungsten wires, on rigid frames under physical tension. Such widely used and commercially available THz polarizers are typically free-standing, with function efficiencies highly reliant on wire spacing constants.^{6,7}

Here, we introduce a thin-film (<10 μm) homogeneous material composed of single-walled carbon nanotubes (SWCNTs) that gives comparable performance to wire-grid technology but has added benefits of (i) broadband THz absorption driven by the inherent one-dimensional (1-D) character of the SWCNTs and (ii) mechanical robustness in diverse operation conditions. In comparison to wire-grid technology, the THz performance of our material is driven not by the precise structure of the conductive wires but rather the inherent anisotropic THz absorption properties of aligned SWCNTs. Although carbon nanomaterials (SWCNTs and graphene) are predicted to be excellent THz materials,^{8–10} previous THz measurements of SWCNTs were performed either on individual SWCNTs or on collective materials not ideally suited for this application. Recently, we demonstrated a collective SWCNT material that behaves as a THz polarizer, with an 80% degree of polarization (DOP) and extinction ratio (ER) of 10 dB—properties below industrial standards due to the nonideal extinction characteristics of the films.¹¹ More

Received: October 26, 2011

Revised: January 4, 2012

Published: January 23, 2012

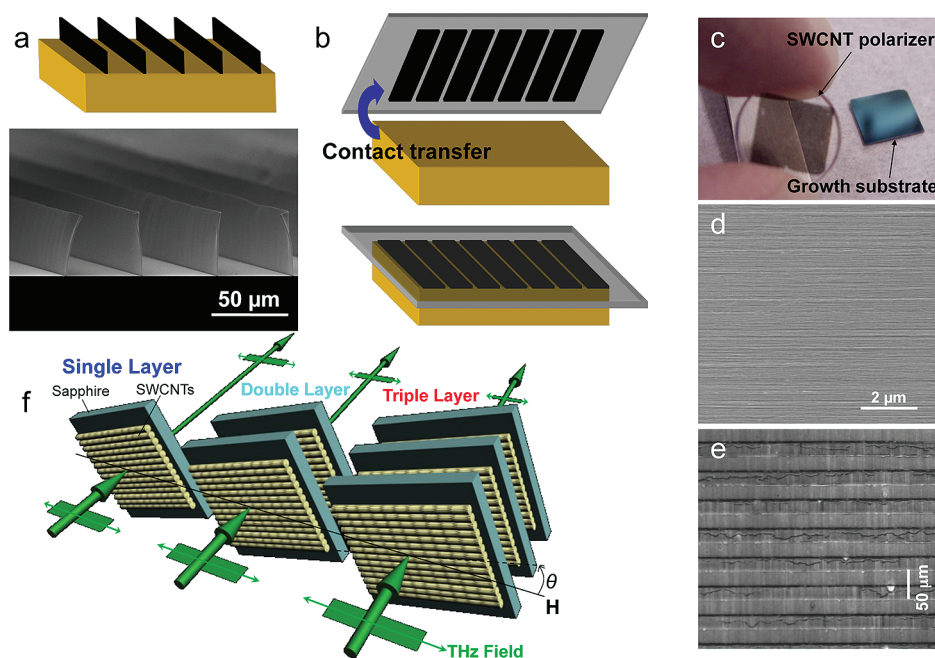


Figure 1. (a) Growth of upright SWCNT lines using patterned catalyst substrates; (b) contact transfer of SWCNT polarizers to transparent sapphire substrates; (c) image showing transferred SWCNT polarizer and growth substrate from which transfer occurred; (d,e) scanning electron microscope and optical microscope images showing the excellent SWCNT alignment inside of the transferred SWCNT structures; and (f) scheme showing the use of multiple SWCNT films to produce high-performance polarizers discussed in this work.

recently, Kyoung et al. reported on a high-performance carbon nanotube THz polarizer by mechanically winding multiwalled carbon nanotubes on a U-shaped polyethylene frame and reached an ER of ~ 37 dB.¹² In this Letter, we report on further advanced SWCNT-based THz polarizers. By utilizing consecutively stacked films of aligned SWCNTs, we achieve here a 99.9% DOP, ER of 30 dB, and broadband performance from ~ 0.4 to 2.2 THz, demonstrating the remarkable utility of aligned SWCNTs for THz applications.

Unlike tedious top-down approaches required to generate precise material structures for wire-grid polarizers, the aligned SWCNT films studied here were produced by natural self-assembly of SWCNTs into densely packed and highly aligned macroscopic materials during SWCNT synthesis. Utilizing optical lithography to define the pitch between lines of catalyst, we then employed water-assisted chemical vapor deposition to grow aligned SWCNTs in high aspect-ratio lines, as shown in Figure 1a. Following growth, we transferred the lines to a sapphire window (Figure 1b,c) to produce a THz polarizer.^{13–17} Figure 1d,e shows scanning electron microscope and optical microscope images, respectively, showing the excellent SWCNT alignment in the transferred structures. To optimize the device performance with respect to extinction, multiple layers were stacked until full extinction of linearly polarized THz radiation was achieved in a configuration where the THz field is parallel to the alignment (see Figure 1f). The benefit of this approach compared to other possible approaches is the simplicity of the contact-transfer process that makes this scalable to large areas. Although the specific growth system utilized in these experiments constrained our growth substrate size to ~ 1 – 1.5 cm², there are no known limitations in this approach that would inhibit scaling to full wafers or even continuous roll-to-roll growth and contact transfer techniques to yield high-throughput production of THz devices.¹⁸

Figure 2a–d shows time-domain waveforms for THz waves transmitted through the reference sapphire substrates (black dashed curves with open circle markers) and the SWCNT films (blue curves for parallel cases and red curves for perpendicular cases), for single and multiple stacks of aligned SWCNT films. For the single SWCNT polarizer in the perpendicular configuration, the transmission was almost that of the blank sapphire reference, suggesting minimal loss.¹¹ For the parallel case, the signal was significantly reduced, suggesting that the absorption of the THz electric field by the nanotubes is strong. As the thickness is increased to include three-film stacks, the THz transmission at the parallel direction became completely attenuated by the polarizer.

Figure 2e–h shows the transmittance spectra calculated after Fourier transformation of the time-domain data in Figure 2a–d in the range of 0.2–2.2 THz. The transmittance was defined as $T = |E_s/E_r|^2$, where E_s and E_r are the complex THz signals in the frequency domain after Fourier transform from their time-domain data for the sample and the reference, respectively. From these four panels, we can more clearly identify the anisotropy. For a thin-film single-SWCNT polarizer with gaps between adjacent lines (Figure 2e), the transmittance is almost 1 in the perpendicular configuration and small (0.2–0.4) in the parallel configuration. This is in contrast to a stack of three films (Figure 2h), where the transmission is still ~ 1 for the perpendicular configuration but 0 throughout the whole frequency range in the parallel configuration. The THz transmittance also decreases with increasing frequency, conflicting with the Drude model valid for conventional metals, such as those tungsten wires for wire-grid THz polarizers. This frequency dependence is consistent with previous far-infrared/THz spectroscopy studies performed on various types of SWCNT samples, showing a robust absorption peak around 4 THz, whose origin is still under debate.^{19–22}

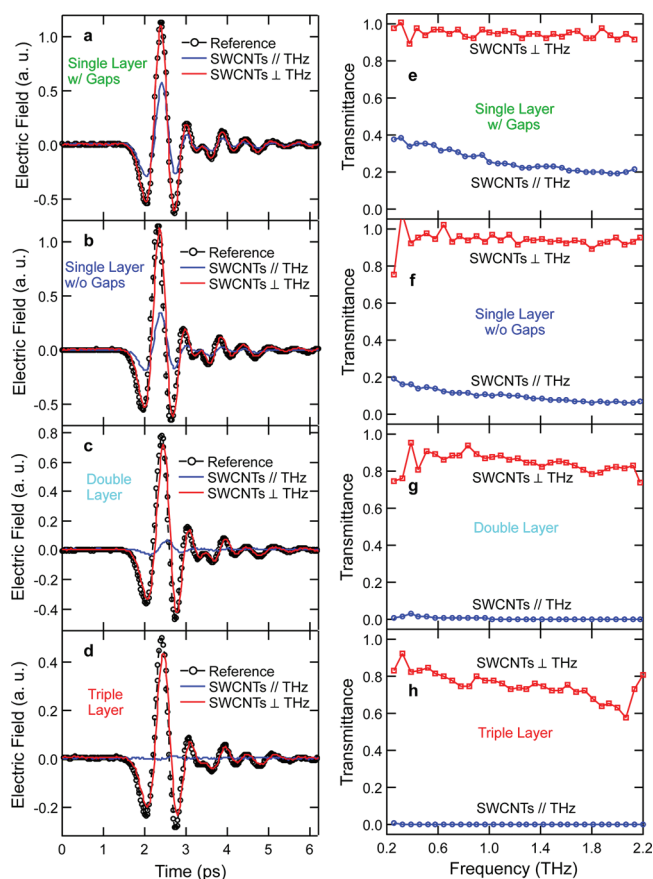


Figure 2. Transmitted THz electric field signals in the time domain for (a) single-layer SWCNT film with gaps; (b) single-layer SWCNT film without gaps; (c) double-layer SWCNT film; and (d) triple-layer SWCNT film. Black dashed lines with open circles are for the reference sapphire substrate, blue solid lines are for samples with THz polarization parallel to the nanotube axis, and red solid lines are for samples with THz polarization perpendicular to the nanotube axis. On the right column, THz transmittance spectra in the 0.2–2.2 THz range are shown for (e) single-layer SWCNT film with gaps; (f) single-layer SWCNT film without gaps; (g) double-layer SWCNT film; and (h) triple-layer SWCNT film. Blue solid lines with open circle markers are for the parallel case, and red solid lines with open square markers are for the perpendicular case.

To elucidate polarizer performance, we calculated the DOP, defined as $DOP = (T_{\perp} - T_{\parallel}) / (T_{\perp} + T_{\parallel})$, and the ER, $ER = T_{\parallel} / T_{\perp}$, where T_{\parallel} is the transmittance for the parallel case, and T_{\perp} is the transmittance for the perpendicular case. As shown in Figure 3a, the DOP value of our SWCNT polarizer increases with the SWCNT film thickness and reaches a value at 99.9% throughout the whole measured frequency range for a triple-stacked film. Figure 3b indicates that the ER value is increasing dramatically with the film thickness, achieving an average value of 33.4 dB in the 0.4–2.2 THz range – 2 orders of magnitude better than the thinner SWCNT films.

In addition to better broadband and DOP than THz wire-grid polarizers, the SWCNT array structures enable versatile operation outside of the THz regime. The thick SWCNT films also exhibit strong mid-infrared and visible polarization responses,^{17,23} allowing their use as anisotropic absorbers in an ultrawide spectral range from the THz to the visible. This enables a complex integration scheme for these materials as optical components in diverse applications utilizing broadband radiation for imaging and/or communication, such as in

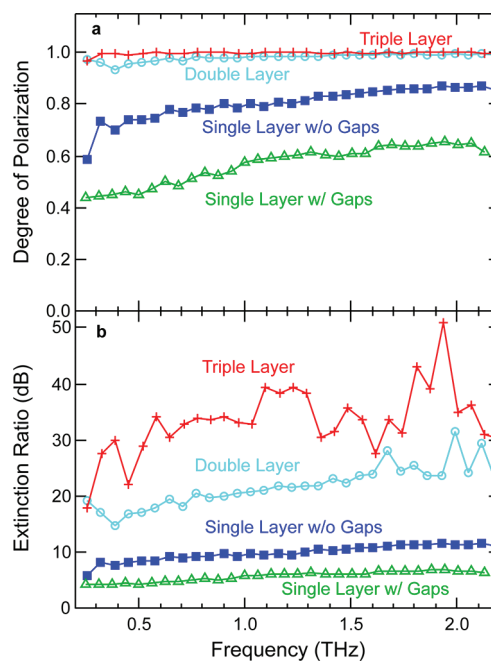


Figure 3. (a) Degree of polarization and (b) extinction ratio of the THz polarizers with different thicknesses as a function of frequency in the 0.2–2.2 THz range. For the optimized triple-layer SWCNT polarizer, the averaged value of the extinction ratio in this frequency range is 33.4 dB.

medical diagnostics. As the transfer process is capable of being scaled to large areas and the carbon nanotube synthetic process depends on cheap carbon precursors and earth-abundant metal catalysts, the latter of which is removed from the SWCNTs prior to making the device, this route represents a high-performance material capable of penetrating the market for THz technology in the future.

In summary, we have synthesized optical polarizers made of highly aligned single-walled carbon nanotube films on sapphire substrates that exhibited remarkable broadband performance in the THz frequency range, with DOP of 99.9% from ~0.4 to 2.2 THz and extinction ratios of up to ~35 dB. This material yields broadband polarization and extinction features that outperform wire-grid polarizers, with multiple additional benefits including robust mechanical structure, a scalable printing process for the SWCNTs, and diverse component operation outside of the THz frequency range. Such materials will be key for the development of the next generation in THz applications and technology.

■ ASSOCIATED CONTENT

Supporting Information

Descriptions of experimental THz measurements and setup and details of sample preparation. This material is available free of charge via the Internet at <http://pubs.acs.org>.

■ AUTHOR INFORMATION

Corresponding Author

* E-mail: kono@rice.edu.

Author Contributions

#These authors contributed equally.

■ ACKNOWLEDGMENTS

This work was supported by the Department of Energy BES Program (through grant no. DE-FG02-06ER46308), the National Science Foundation (through grant no. OISE-0968405), and the Robert A. Welch Foundation (through grant no. C-1509). We thank Michelle Z. Jin for technical assistance.

■ REFERENCES

- (1) *Sensing with Terahertz Radiation*; Mittleman, D., Ed.; Springer-Verlag: Berlin, Heidelberg, Germany, 2002.
- (2) Tonouchi, M. *Nat. Photonics* **2007**, *1*, 97–105.
- (3) Chen, H.-T.; Padilla, W. J.; Cich, M. J.; Azad, A. K.; Averitt, R. D.; Taylor, A. J. *Nat. Photonics* **2009**, *3*, 148–151.
- (4) Qin, Q.; Williams, B. S.; Kumar, S.; Reno, J. L.; Hu, Q. *Nat. Photonics* **2009**, *3*, 732–737.
- (5) Liu, J.; Dai, J.; Chin, S. L.; Zhang, X.-C. *Nat. Photonics* **2010**, *4*, 627–631.
- (6) Costley, A. E.; Hursey, K. H.; Neill, G. F.; Ward, J. M. *J. Opt. Soc. Am.* **1977**, *67*, 979–981.
- (7) Ade, P. A. R.; Costley, A. E.; Cunningham, C. T.; Mok, C. L.; Neill, G. F.; Parker, T. J. *Infrared Phys.* **1979**, *19*, 599–601.
- (8) Kibis, O. V.; Rosenau da Costa, M.; Portnoi, M. E. *Nano Lett.* **2007**, *7*, 3414–3417.
- (9) Ryzhii, V.; Ryzhii, M.; Otsuji, T. *J. Appl. Phys.* **2007**, *101*, 083114.
- (10) Mikhailov, S. A. *Europhys. Lett.* **2007**, *79*, 27002.
- (11) Ren, L.; Pint, C. L.; Booshehri, L. G.; Rice, W. D.; Wang, X.; Hilton, D. J.; Takeya, K.; Kawayama, I.; Tonouchi, M.; Hauge, R. H.; Kono, J. *Nano Lett.* **2009**, *9*, 2610–2613.
- (12) Kyoung, J.; Jang, E.-Y.; Lima, M. D.; Park, H.-R.; Robles, R.-O.; Lepro, X.; Kim, Y.-H.; Baughman, R. H.; Kim, D.-S. *Nano Lett.* **2011**, *11* (10), 4227–4231.
- (13) Pint, C. L.; Xu, Y.-Q.; Pasquali, M.; Hauge, R. H. *ACS Nano* **2008**, *2*, 1871–1878.
- (14) Pint, C. L.; Pheasant, S. T.; Pasquali, M.; Coulter, K. E.; Schmidt, H. K.; Hauge, R. H. *Nano Lett.* **2008**, *8*, 1879–1883.
- (15) Pint, C. L.; Pheasant, S. T.; Nicholas, N.; Horton, C.; Hauge, R. H. *J. Nanosci. Nanotechnol.* **2008**, *8*, 6158–6164.
- (16) Pint, C. L.; Pheasant, S. T.; Parra-Vasquez, A. N. G.; Horton, C.; Xu, Y.; Hauge, R. H. *J. Phys. Chem. C* **2009**, *113*, 4125–4133.
- (17) Pint, C. L.; Xu, Y.-Q.; Moghazy, S.; Cherukuri, T.; Alvarez, N. T.; Hároz, E. H.; Mahzooni, S.; Doorn, S. K.; Kono, J.; Pasquali, M.; Hauge, R. H. *ACS Nano* **2010**, *4*, 1131–1145.
- (18) de Villoria, R. G.; Hart, A. J.; Wardle, B. L. *ACS Nano* **2011**, *5*, 4850–4857.
- (19) Ugawa, A.; Rinzler, A. G.; Tanner, D. B. *Phys. Rev. B* **1999**, *60*, R11305–R11308.
- (20) Itkis, M. E.; Niyogi, S.; Meng, M. E.; Hamon, M. A.; Hu, H.; Haddon, R. C. *Nano Lett.* **2001**, *2*, 155–159.
- (21) Akima, N.; Iwasa, Y.; Brown, S.; Barbour, A. M.; Cao, J.; Musfeldt, J. L.; Matsui, H.; Toyota, N.; Shiraishi, M.; Shimoda, H.; Zhou, O. *Adv. Mater.* **2006**, *18*, 1166–1169.
- (22) Kampfrath, T.; von Volkmann, K.; Aguirre, C. M.; Desjardins, P.; Martel, R.; Krenz, M.; Frischkorn, C.; Wolf, M.; Perfetti, L. *Phys. Rev. Lett.* **2008**, *101*, 267403.
- (23) Booshehri, L. G.; Pint, C. L.; Sanders, G. D.; Ren, L.; Sun, C.; Hároz, E. H.; Kim, J.-H.; Yee, K.-J.; Lim, Y.-S.; Hauge, R. H.; Stanton, C. J.; Kono, J. *Phys. Rev. B* **2011**, *83*, 195411.